Supplementary Information (SI) of Simultaneous Elimination of Cationic Uranium(VI) and Anionic Rhenium(VII) by Graphene Oxide-Poly(ethyleneimine) Macrostructures: a Batch, XPS, EXAFS, and DFT Combined Study

Zhi-Wei Huang [a,b], Zi-Jie Li [a], Qun-Yan Wu [a], Li-Rong Zheng [c], Li-Min Zhou [b], Zhi-Fang Chai [d], Xiao-Lin Wang [e], Wei-Qun Shi [a*]

[a] Laboratory of Nuclear Energy Chemistry and Key Laboratory for Biomedical Effects of Nanomaterials and Nanosafety, Institute of High Energy Physics, Chinese Academy of Sciences, Beijing, 100049, China

[b] School of Chemistry, Biological and Materials Sciences, East China University of Technology, Nanchang 330013, China

[c] Beijing Synchrotron Radiation Facility, Institute of High Energy Physics, Chinese Academy of Sciences, Beijing, 100049, China

[d] School of Radiological and Interdisciplinary Sciences (RAD-X), and Collaborative Innovation Center of Radiation Medicine of Jiangsu Higher Education Institutions, Soochow University, Suzhou 215123, China

[e] Institute of Nuclear Physics and Chemistry, China Academy of Engineering Physics, Mianyang, Sichuan, 621900, China

* Corresponding authors: E-mail: shiwq@ihep.ac.cn (W.Q. Shi). The first two authors contributed equally to this work.

EXAFS models for U(VI)-loaded GO-PEI samples. The paths of U-O_{ax}, MS of U-O_{ax}, U-O/N_{eq} were fitted from the crystal structure of $[UO_2][NH_2]_2O_2[H_2O]_3$, the U-$C_1$ and U-U paths were fitted from the crystal structures of $Na_4UO_2(CO_3)_3$ and schoepite, respectively, whereas the U-C_2 shell at 3.45 and 3.50 Å was from $UO_2(C_6H_8O_4)(C_{10}H_8N_2)$ and UO_2(dbsf)(phen) (dbsf: 4,4'-dicarboxybiphenyl sulfone, phen: 1,10-phenanthroline), respectively.

Table S1. Description of the U EXAFS model for the treated GO-PEI samples with uranium. The variables in the model are marked with bold type.

Path	R_{eff} **(Å)**	***CN***	ΔR **(Å)**	σ^2 **(Å^2)**	ΔE **(eV)**
U-O_{ax}	1.81	2	ΔR_{Oax}	σ^2_{Oax}	ΔE_0

U-O_{ax1}-O_{ax2}	3.61	2	$2{\cdot}\Delta R_{Oax}$	$2{\cdot}\sigma^2_{Oax}$	ΔE_0
U-O_{ax1}-U-O_{ax2}	3.61	2	$2{\cdot}\Delta R_{Oax}$	$2{\cdot}\sigma^2_{Oax}$	ΔE_0
U-O_{ax1}-U-O_{ax1}	3.61	2	$2{\cdot}\Delta R_{Oax}$	$4{\cdot}\sigma^2_{Oax}$	ΔE_0
U-O/N_{eq1}	2.31	$\boldsymbol{N_{Oeq1}}$	$\boldsymbol{\Delta R_{Oeq1}}$	$\boldsymbol{\sigma^2_{Oeq1}}$	ΔE_0
U-O/N_{eq2}	2.50	6/5-N_{Oeq1}	$\boldsymbol{\Delta R_{O/Neq2}}$	σ^2_{Oeq1}	ΔE_0
U-C_1	2.86	$\boldsymbol{N_{C1}}$	$\boldsymbol{\Delta R_{C1}}$	0.004	ΔE_0
U-C_2	3.45/3.50	$\boldsymbol{N_{C2}}$	$\boldsymbol{\Delta R_{C2}}$	0.004	ΔE_0
U-U	3.83	$\boldsymbol{N_U}$	$\boldsymbol{\Delta R_U}$	0.004	ΔE_0

Pseudo-first-order and pseudo-second-order kinetic models and fitting results. The adsorption kinetic data were fitted by using pseudo-first-order and pseudo-second-order models, and their linear form can be expressed as:

Pseudo-first-order: $\ln(q_e - q_t) = lnq_e - k_1 t$

Pseudo-second-order: $\frac{t}{q_t} = \frac{1}{k_2 q_e^2} + \frac{1}{q_e} t$

where q_e and q_t represent the amount of metal adsorbed at equilibrium and time t, respectively; k_1 and k_2 are the rate constants of the two models, respectively.

Table S2. pH values of the solutions with different molar ratios of Na_2CO_3 to UO_2^{2+}, C_0(U) = 100 mg/L.

molar ratio (Na_2CO_3:$UO_2(NO_3)_2$)	0:1	1:1	2:1	3:1
Solution pH	4.20	5.42	6.64	8.51

Table S3. Kinetic parameters of the adsorption of U(VI)/Re(VII) on the GO-PEI.

		Pseudo-first-order				Pseudo-second-order		
	pH	q_e exp (mg/g)	k_1 (/min)	q_e cal (mg/g)	R^2	k_2 ($\times10^{-3}$g/mg/min)	q_e cal (mg/g)	R^2
U	3.5	32.12	0.109	28.45	0.937	5.239	30.49	**0.983**

	5.0	218.66	0.170	204.71	0.949	1.273	215.63	**0.991**
	8.3 (10ppm)	26.04	0.947	25.81	0.999	0.384	25.89	0.999
Re	3.5	151.00	0.772	151.38	0.998	54.08	151.80	**0.999**
	6.0	61.81	0.135	56.57	0.938	3.32	60.28	**0.984**

Adsorption isotherms and fitting results

The adsorption isotherm data were fitted by using Langmuir and Freundlich models The Langmuir and Freundlich isotherm models are expressed as:

Langmuir: $$\frac{C_e}{q_e} = \frac{C_e}{q_m} + \frac{1}{q_m k_L}$$

Freundlich: $$lnq_e = lnk_F + \frac{1}{n} lnC_e$$

where q_e and C_e represent the adsorption capacity and the concentration of metal ions at equilibrium condition respectively; k_L is the Langmuir isotherm constant and q_m is the maximum adsorption capacity of the adsorbent. k_F is the Freundlich isotherm constant and $1/n$ is related to the heterogeneity parameter of the sorbent.

Table S4. Isotherm model parameters for the adsorption of U(VI) and Re(VII) on GO-PEI at pH 3.5 and 5.0.

			Langmuir Model			Freundlich Model		
Adsorbate	pH	$NaClO_4$ concentration	q_m (mg/g)	k_L (L/mg)	R^2	k_F (mg/g)	n	R^2
U	3.5	0 M	75.1	0.010	0.966	1.00	1.452	**0.990**
	5.0	0 M	555.8	0.297	0.931	192.6	3.639	**0.991**
Re	3.5	0 M	458.89	0.010	0.992	11.138	1.505	0.990
		0.01 M	310.85	0.001	0.996	0.665	1.132	0.995
		0.1 M	54.64	0.018	0.985	1.397	1.382	0.999
	6.0	0 M	396.43	0.003	0.999	2.582	1.268	0.999

0.01 M	219.39	0.001	0.998	0.299	1.111	0.999

Table S5. Adsorption capacities of various adsorbents for U(VI) as reported.

Adsorbents	Experimental conditions	Adsorption capacity	References
GO	pH 4.0, *RT*	299 mg/g	[1]
Amidoximated Fe_3O_4@GO	pH 5.0, *T*=298 K	284.9 mg/g	[2]
Polyaniline/GO	pH 3.0, *T*=298 K	245.65 mg/g	[3]
PEI/Spirulina	pH 5.0, *T*=298 K	279.5 mg/g	[4]
Titanate nanotubes	pH 5.0, *T*=298 K	333mg/g	[5]
Carbonaceous Nanofibers	pH 4.5, *T*=298K	125mg/g	[6]
Vanadium Carbide MXene	pH 5.0, *RT*	174mg/g	[7]
GO-PEI	pH 3.5, *RT*	75.1 mg/g	This study
	pH 5.0, *RT*	629.5 mg/g	

Table S6. Simultaneous adsorption of coexisting metal ions in original seawater on the GO-PEI. Contact time = 3 h, m/V = 0.2 g/L.

Element	C_0 (mg/L)	C_f (mg/L)	% removal
Na	9897.14	9871.11	0.3%
Mg	1373.67	1370.81	0.2%
Sr	8.07	7.97	1.2%
	C_0 (μg/L)	C_f (μg/L)	
Ni	17.11	15.39	10.1%
V	2.29	1.27	44.5%
Zn	10.21	8.37	18.0%
Mo	5.11	4.42	13.5%
Al	15.23	12.35	18.9%

Table S7. Alternative structural parameters around uranium in U_pH5.0 and

U_pH8.3_1 derived from EXAFS analyses by constraining the sum of *CN* of equatorial oxygens/nitrogens to be 5 [b].

Sample	Shell	*CN*	*R* (Å)	σ^2 (Å^2)	ΔE_0 (eV)[d]	R_f, Red-χ^2
U_pH5.0	U-O_{ax}	2 [a]	1.82(0)	0.003(0)	14.8(1.0)	6.0×10^{-5}, 11.5
	U-O/N_{eq1}	2.7(4) [b]	2.39(2)	0.007(2) [c]		
	U-O/N_{eq2}	2.3 [b]	2.55(2)			
	U-C_1	1.4(5)	2.93(2)	0.004 [a]		
	U-C_2	3.0(1.0)	3.48(2)	0.005 [a]		
U_pH8.3_1	U-O_{ax}	2 [a]	1.82(0)	0.003(0)	13.7(1.0)	8.6×10^{-5}, 10.4
	U-O/N_{eq1}	2.9(6) [b]	2.41(2)	0.005(2) [c]		
	U-O/N_{eq2}	2.1 [b]	2.54(3)			
	U-C_1	1.8(5)	2.93(2)	0.004 [a]		
	U-C_2	3.0(1.1)	3.48(2)	0.004 [a]		

Note: CN: coordination number; *R*: bond distance; σ^2: Debye-Waller factor; R_f, Red-χ^2: quality of fit as defined in the literature; Number in parentheses present the errors in the last digit. [a] Value fixed during the fit; [c] σ^2 was allowed to vary but linked for two equatorial O/N shells; [d] ΔE_0 was allowed to vary but lined for all paths

Table S8. Structural parameters for aqueous ReO_4^- and Re_pH3.5 derived from EXAFS analyses. FT^{-1} range from 3.9 to 14.8 $Å^{-1}$ and FT from 1.0 to 1.8 Å.

Sample	Shell	*CN*	*R* (Å)	σ^2 (Å^2)	ΔE_0 (eV)	R_f, Red-χ^2
ReO_4^- (aq)	Re-O	4	1.74(1)	0.001(1)	10.5(2.6)	5.8×10^{-5}, 171
Re_pH3.5	Re-O	3.9	1.74(1)	0.001(1)	11.4(3.3)	2.0×10^{-4}, 712

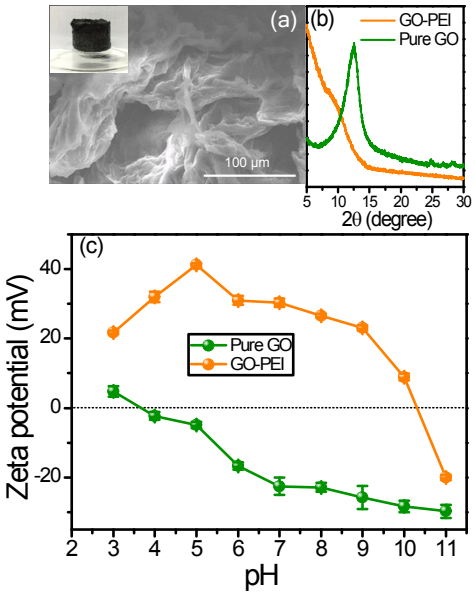

Figure S1. Characterizations of the pure GO and GO-PEI. (a) The GO-PEI SEM, the inset in the top left corner is an image of the GO-PEI; (b) XRD patterns, and (c) Zeta potentials.

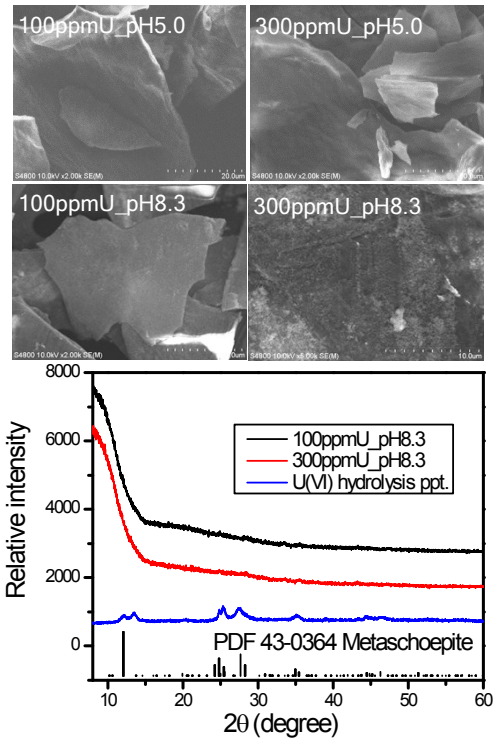

Figure S2. SEM and XRD characterizations of the treated GO-PEI with uranium adsorbed.

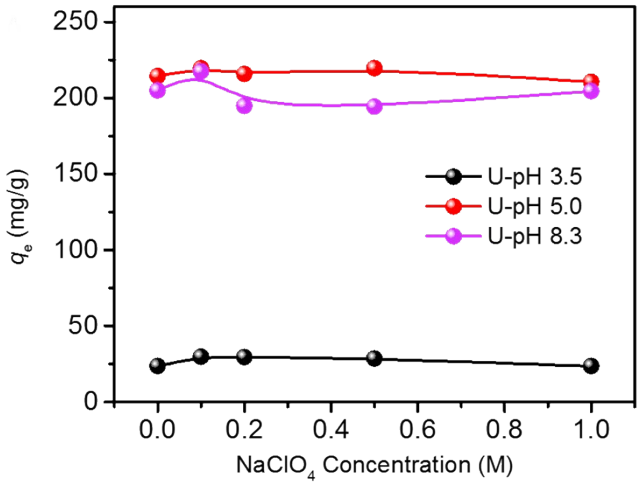

Figure S3. Effect of ionic strength on the U(VI) adsorption on GO-PEI, C_0(U)=100 mg/L, m/V=0.4 g/L.

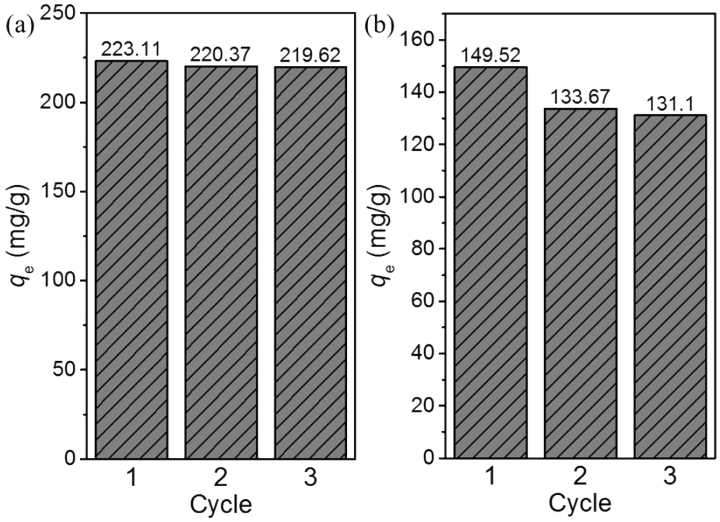

Figure S4. (a) Reusability of the GO-PEI in the removal of U(VI). m/V=0.4 g/L, C_0(U)=100 mg/L, pH=5.0. A 0.1 M HNO_3 solution was utilized to desorb the adsorbed U(VI). (b) Reusability of the GO-PEI in the removal of Re(VII). m/V=0.4 g/L, C_0(Re)=100 mg/L, pH=3.5. A 0.1 mM NaOH solution was utilized to desorb the adsorbed Re(VII).

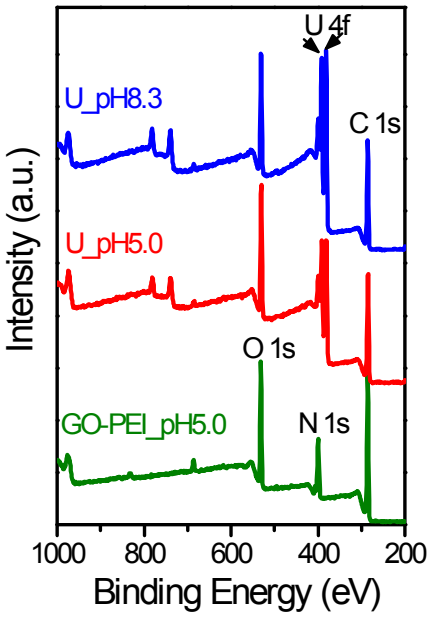

Figure S5. XPS survey spectra of the fresh GO-PEI, U_pH5.0, and U_pH8.3.

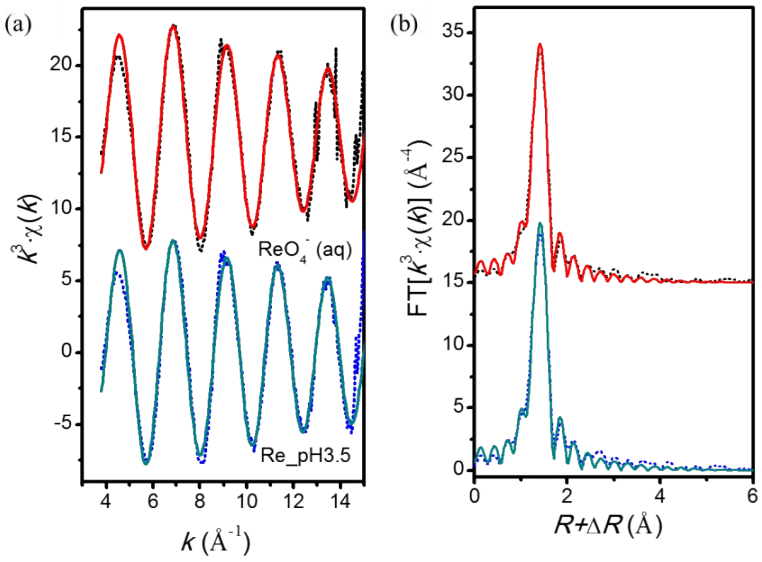

Figure S6. (a) The k^3-weighted Re L_{III}-edge EXAFS spectra of the ReO_4^- (aq) reference and the GO-PEI sample after rhenium adsorption at pH 3.5 (Re_pH3.5), and (b) corresponding FT spectra. C_0(Re)=100 mg/L, m/V=0.4 g/L, dotted lines: experimental data; solid lines: fitted data.

Theoretical computational details

In order to investigate the coordination modes of U(VI)/Re(VII) with the GO-PEI

at the molecular level, the structures of U(VI)/Re(VII) complexes with PEI were optimized using density functional theory (DFT). To save computational efficiency, a unit of PEI was chosen as a computational model. All structures were optimized using the hybrid exchange-correlation function B3LYP method[8] with the Gaussian 09 program.[9] The quasi-relativistic pseudo-potential ECP60MWB and associated ECP60MWB valence basis sets were used to describe for U and Re atoms,[10,11] the 6-31G(d) basis set was used for the other light atoms H, C, N, and O. To confirm the adsorption mechanism of Re(VII) ion, the fragment calculations were carried out in the ADF program,[12] which could supply an energetic decomposition of the PEI-Re(VII) interaction. The BP86 functional and the Slater type orbital (STO) basis set with the quality of the triple-zeta plus polarization (TZP) basis set were used,[13] without the frozen core. The interaction energy (ΔE_{int}) between two fragments is defined as the sum of three terms: $\Delta E_{int}=\Delta E_{pauli} + \Delta E_{es} + \Delta E_{orb}$. Here, ΔE_{pauli} and ΔE_{es} are Pauli repulsive interaction and electrostatic interaction energy between the fragments, respectively. The ΔE_{orb} gives the stabilizing orbital interaction.

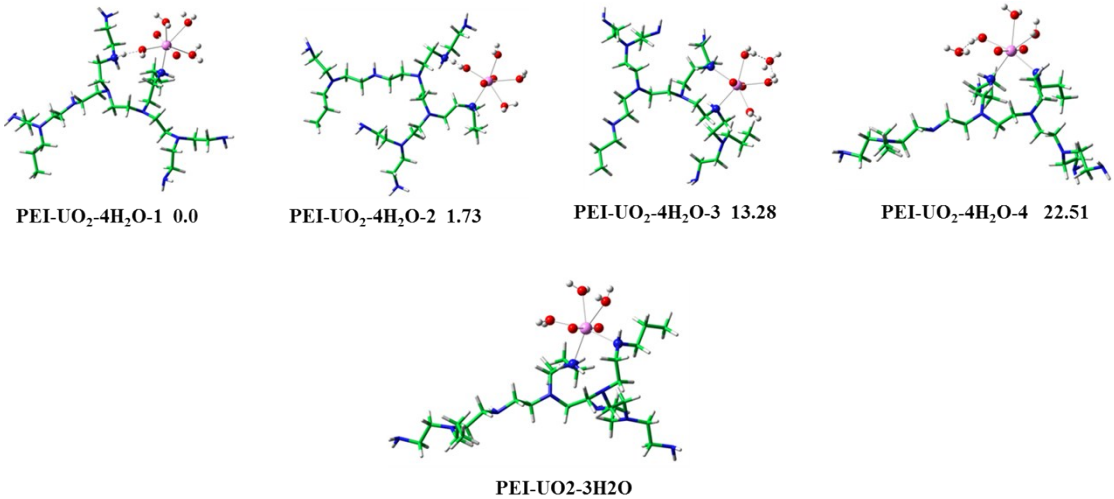

Figure S7. Structures of the complexes PEI-UO_2-nH_2O (n=3,4) and the relative electronic energies (kcal/mol) are provided.

Table S9. Calculated U-N, U-O and hydrogen bond lengths (Å) and $O_{ax}UO_{ax}$ bond

angles (degree) for the complexes PEI-UO_2-nH_2O (n=3,4)[a].

	U-N	U-N	U-O_w	U-O_w	U-O_w	U-O_w	U-O_{ax}	U-O_{ax}	H-bond	$O_{ax}UO_{ax}$
PEI-UO_2-$4H_2O$-1	2.625	–	2.618	2.653	2.584	2.218	1.781	1.778	1.772	177.9
PEI-UO_2-$4H_2O$-2	2.631	–	2.610	2.703	2.585	2.229	1.779	1.778	1.817	177.3
PEI-UO_2-$4H_2O$-3	2.622	2.653	2.547	2.541	2.541	–	1.774	1.779	1.844/ 1.810	174.8
PEI-UO_2-$4H_2O$-4	2.582	2.665	2.590	2.654	2.495	–	1.787	1.772	1.657	176.5
PEI-UO_2-$3H_2O$	2.590	2.630	2.630	2.629	2.587	–	1.776	1.774	–	178.6

[a] N denotes the nitrogen atom of PEI molecule, O_w denotes the oxygen atom of water molecules.

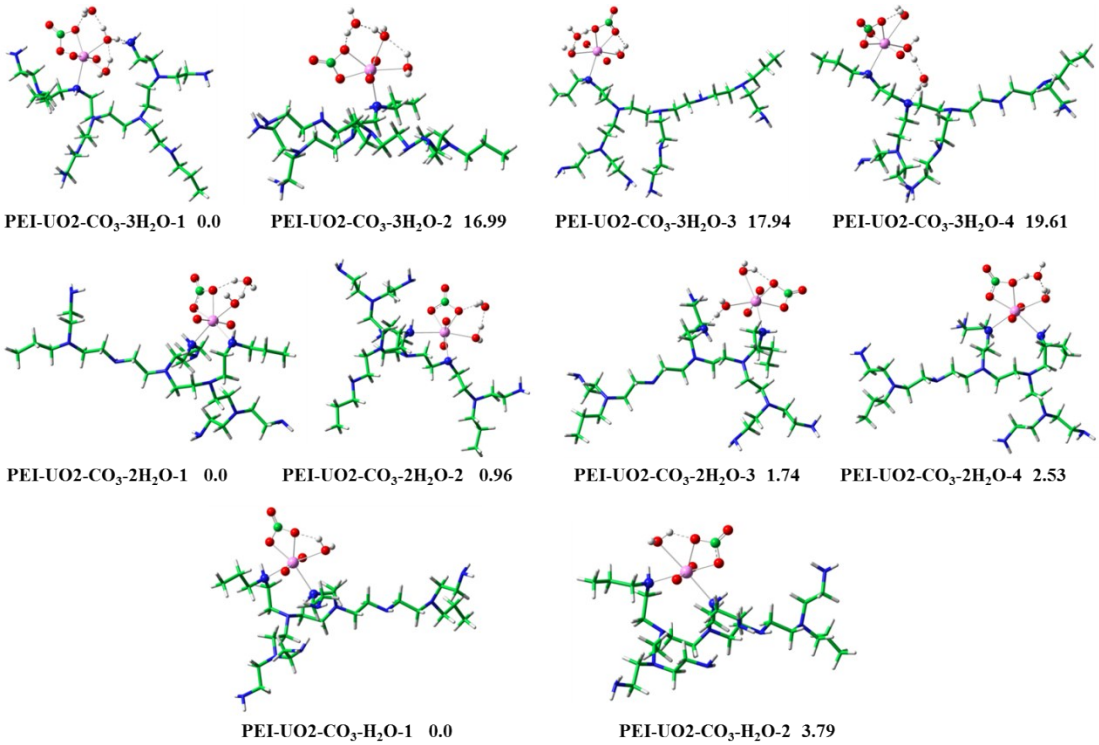

Figure S8. Structures of the complexes PEI-UO_2-CO_3-nH_2O (n=1-3) and the relative electronic energies (kcal/mol) are provided.

Table S10. Calculated U-N, U-O, U-C and hydrogen bond lengths (Å) and $O_{ax}UO_{ax}$ bond angles (degree) for the complexes PEI-UO_2-CO_3-nH_2O (n=1-3).[a]

	U-N	U-N	U-O_c	U-O_c	U-O_w	U-O_w	U-O_{ax}	U-O_{ax}	U-C	H-bond	$O_{ax}UO_{ax}$
PEI-UO_2-CO_3-$3H_2O$-1	2.655	–	2.240	2.301	2.525	2.694	1.788	1.792	2.771	1.824/1.691/ 1.661/1.763	171.0
PEI-UO_2-CO_3-$3H_2O$-2	2.665	–	2.233	2.288	2.652	2.609	1.788	1.787	2.771	1.604/1.731/ 1.992	169.4
PEI-UO_2-CO_3-$3H_2O$-3	2.695	–	2.285	2.289	2.600	2.512	1.781	1.789	2.803	1.613/1.742/ 1.889	170.9
PEI-UO_2-CO_3-$3H_2O$-4	2.700	–	2.235	2.272	2.570	2.636	1.791	1.788	2.763	1.657/1.767/ 1.887	170.9

PEI-UO_2-CO_3-2H_2O-1	2.695	2.771	2.272	2.299	2.575	–	1.786	1.785	2.800	1.626/1.758	170.6
PEI-UO_2-CO_3-2H_2O-2	2.762	2.720	2.276	2.299	2.524	–	1.790	1.783	2.800	1.619/1.759	171.1
PEI-UO_2-CO_3-2H_2O-3	2.675	–	2.245	2.284	2.621	2.502	1.794	1.793	2.776	1.615/1.842	168.5
PEI-UO_2-CO_3-2H_2O-4	2.668	2.748	2.271	2.295	2.582	–	1.789	1.786	2.795	1.625/1.736	169.7
PEI-UO_2-CO_3-H_2O-1	2.681	2.698	2.254	2.280	2.638	–	1.789	1.793	2.782	1.828	170.5
PEI-UO_2-CO_3-H_2O-2	2.684	2.734	2.268	2.279	2.704	–	1.787	1.784	2.792	1.787	169.6

[a] O_c denotes the oxygen atom of carbonate group, C denotes the carbon atom of carbonate group.

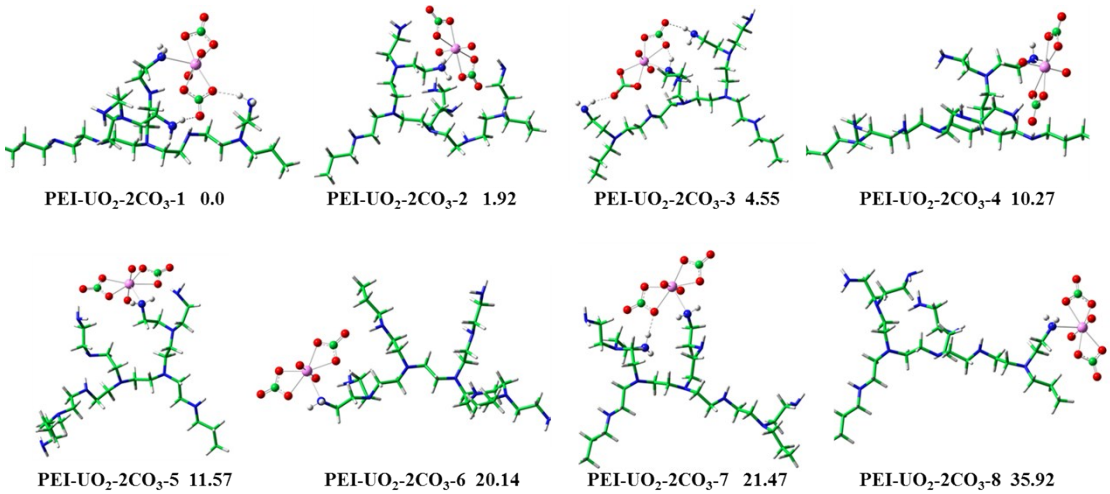

Figure S9. Structures of the complexes PEI-UO_2-$2CO_3$ and the relative electronic energies (kcal/mol) are provided.

Table S11. Calculated U-N, U-O and U-C bond lengths (Å) and $O_{ax}UO_{ax}$ bond angles (degree) for the complexes PEI-UO_2-$2CO_3$.

	U-N	U-O_c	U-O_c	U-O_c	U-O_c	U-O_{ax}	U-O_{ax}	U-C	U-C	$O_{ax}UO_{ax}$
PEI-UO_2-$2CO_3$-1	2.636	2.372	2.280	2.434	2.387	1.804	1.811	2.809	2.852	175.3
PEI-UO_2-$2CO_3$-2	2.584	2.370	2.340	2.371	2.419	1.810	1.804	2.821	2.844	177.6
PEI-UO_2-$2CO_3$-3	2.709	2.419	2.315	2.402	2.334	1.803	1.807	2.823	2.831	175.4
PEI-UO_2-$2CO_3$-4	2.644	2.456	2.362	2.375	2.288	1.805	1.810	2.854	2.811	176.1
PEI-UO_2-$2CO_3$-5	2.634	2.432	2.320	2.416	2.321	1.805	1.808	2.834	2.852	174.6
PEI-UO_2-$2CO_3$-6	2.713	2.428	2.350	2.394	2.289	1.804	1.818	2.846	2.824	173.8
PEI-UO_2-$2CO_3$-7	2.618	2.337	2.439	2.300	2.387	1.810	1.808	2.821	2.854	175.2
PEI-UO_2-$2CO_3$-8	2.650	2.401	2.334	2.398	2.308	1.812	1.811	2.828	2.837	175.4

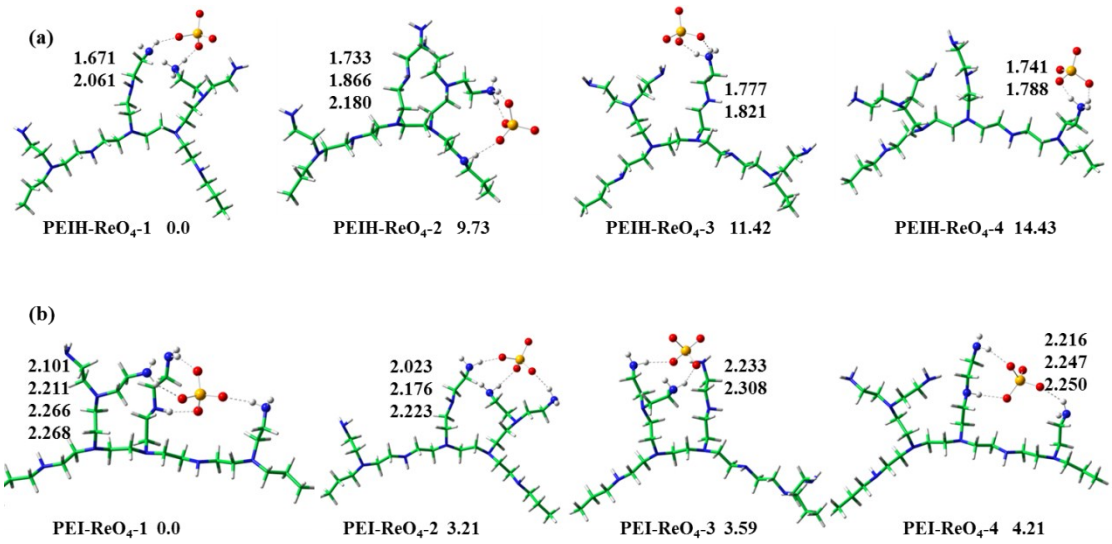

Figure S10. Structures of the protonated PEIH-ReO_4 (a) and PEI-ReO_4 (b) complexes as well as the relative electronic energies (kcal/mol) and hydrogen bonding lengths (Å) are provided.

Table S12. Interaction energies (kcal/mol) and energy decompositions of the Re(VII) and PEI/protonated PEI interactions at the BP86/TZP level of theory.

Complexes	ΔE_{int}	ΔE_{Pauli}	ΔE_{es}	ΔE_{orb}
PEI-ReO_4	-16.99	16.21	-21.22	-11.98
PEIH-ReO_4	-100.53	33.91	-102.94	-31.51

REFERENCES

1 Z. J. Li, F. Chen, L. Y. Yuan, Y. L. Liu, Y. L. Zhao, Z. F. Chai and W. Q. Shi, Uranium(VI) adsorption on graphene oxide nanosheets from aqueous solutions. *Chem. Eng. J.,* 2012, **210**, 539-546.

2 Y. G. Zhao, J. X. Li, S. W. Zhang, H. Chen and D. D. Shao, Efficient enrichment of uranium(VI) on amidoximated magnetite/graphene oxide composites. *RSC Adv.,* 2013, **3**, 18952-18959.

3 Y. B. Sun, D. D. Shao, C. L. Chen, S. B. Yang and X. K. Wang, Highly efficient enrichment of radionuclides on graphene oxide-supported polyaniline. *Environ. Sci. Technol.,* 2013, **47**, 9904-9910.

4 G. Bayramoglu, A. Akbulut and M. Y. Arica, Study of polyethyleneimine- and amidoxime-functionalized hybrid biomass of Spirulina (Arthrospira) platensis for adsorption of uranium (VI) ion. *Environ. Sci. Pollut. R.,* 2015, **22**, 17998-18010.

5 W. Liu, X. Zhao, T. Wang, D. Y. Zhao and J. R. Ni, Adsorption of U(VI) by multilayer titanate nanotubes: Effects of inorganic cations, carbonate and natural organic matter. *Chem. Eng. J.,* 2016, **286**, 427-435.

6 Y. B. Sun, Z. Y. Wu, X. X. Wang, C. C. Ding, W. C. Cheng, S. H. Yu and X. K. Wang,

Macroscopic and microscopic investigation of U(VI) and Eu(III) adsorption on carbonaceous nanofibers. *Environ. Sci. Technol.,* 2016, **50**, 4459-4467.

7 L. Wang, L.-Y. Yuan, K. Chen, Y.-J. Zhang, Q. Deng, S. Du, Q. Huang, L. Zheng, J. Zhang and Z. Chai, Loading actinides in multi-layered structures for nuclear waste treatment: the first case study of uranium capture with vanadium carbide MXene. *ACS Appl. Mater. Inter.,* 2016.

8 C. T. Lee, W. T. Yang and R. G. Parr, Development of the Colle-Salvetti correlation-energy formula into a functional of the electron density. *Phys. Rev. B,* 1988, **37**, 785-789.

9 M. J. Frisch, G. W. Trucks, H. B. Schlegel, G. E. Scuseria, M. A. Robb, J. R. Cheeseman, G. Scalmani, V. Barone, B. Mennucci, G. A. Petersson, H. Nakatsuji, M. Caricato, X. Li, H. P. Hratchian, A. F. Izmaylov, J. Bloino, G. Zheng, J. L. Sonnenberg, M. Hada, M. Ehara, K. Toyota, R. Fukuda, J. Hasegawa, M. Ishida, T. Nakajima, Y. Honda, O. Kitao, H. Nakai, T. Vreven, J. A. Montgomery Jr., J. E. Peralta, F. Ogliaro, M. J. Bearpark, J. Heyd, E. N. Brothers, K. N. Kudin, V. N. Staroverov, R. Kobayashi, J. Normand, K. Raghavachari, A. P. Rendell, J. C. Burant, S. S. Iyengar, J. Tomasi, M. Cossi, N. Rega, N. J. Millam, M. Klene, J. E. Knox, J. B. Cross, V. Bakken, C. Adamo, J. Jaramillo, R. Gomperts, R. E. Stratmann, O. Yazyev, A. J. Austin, R. Cammi, C. Pomelli, J. W. Ochterski, R. L. Martin, K. Morokuma, V. G. Zakrzewski, G. A. Voth, P. Salvador, J. J. Dannenberg, S. Dapprich, A. D. Daniels, Ö. Farkas, J. B. Foresman, J. V. Ortiz, J. Cioslowski and D. J. Fox *Gaussian 09*, Gaussian, Inc.: Wallingford, CT, USA, 2009.

10 J. M. L. Martin and A. Sundermann, Correlation consistent valence basis sets for use with the Stuttgart–Dresden–Bonn relativistic effective core potentials: The atoms Ga–Kr and In–Xe. *J. Chem. Phys.,* 2001, **114**, 3408-3420.

11 M. Hulsen, A. Weigand and M. Dolg, Quasirelativistic energy-consistent 4f-in-core pseudopotentials for tetravalent lanthanide elements. *Theor. Chem. Acc.,* 2009, **122**, 23-29.

12 G. te Velde, F. M. Bickelhaupt, E. J. Baerends, C. Fonseca Guerra, S. J. A. van Gisbergen, J. G. Snijders and T. Ziegler, Chemistry with ADF. *J. Comput. Chem.,* 2001, **22**, 931-967.

13 E. Van Lenthe and E. J. Baerends, Optimized Slater-type basis sets for the elements 1–118. *J. Comput. Chem.,* 2003, **24**, 1142-1156.